




FNF-12, a novel benzylidene-chromanone derivative, attenuates inflammatory response in in vitro and in vivo asthma models mediated by M2-related Th2 cytokines via MAPK and NF- κ B signaling

Mohammad Abohassan¹ · Mesfer Al Shahrani¹ · Mohammad Y. Alshahrani¹ · Naseem Begum¹ · Suresh Radhakrishnan³ · Prasanna Rajagopalan^{1,2} 

Received: 22 March 2021 / Revised: 2 August 2021 / Accepted: 23 August 2021 / Published online: 1 September 2021
© Maj Institute of Pharmacology Polish Academy of Sciences 2021

Abstract

Background and aim This study evaluates a novel benzylidene-chromanone derivative, FNF-12, for efficacy in in vitro and in vivo asthma models.

Methods Rat basophilic leukemia (RBL-2H3) and acute monocytic leukemia (THP-1)-derived M2 macrophages were used. Human whole blood-derived neutrophils and basophils were employed. Flow cytometry was used for studying key signalling proteins. Platelet activation factor (PAF)-induced asthma model in guinea pigs was used for in vivo studies.

Results The chemical structure of FNF-12 was confirmed with proton-nuclear mass resonance (NMR) and mass spectroscopy. FNF-12 controlled degranulation in RBL-2H3 cells with an IC₅₀ value of 123.7 nM and inhibited TNF- α release from these cells in a dose-responsive way. The compound effectively controlled the migration and elastase release in activated neutrophils. IC₅₀ value in the Fc ϵ RI-basophil activation assay was found to be 205 nM. FNF-12 controlled the release of lipopolysaccharide (LPS)-induced interleukin-10, I-309/CCL1 and MDC/CCL22 in THP-1 derived M2 macrophages. The compound suppressed LPS-induced mitogen activated protein kinase (MAPK)-p-p38 and nuclear factor kappa B(NF- κ B)-p-p65 expression in these cells. A dose-dependent decrease in the accumulation of total leucocytes, eosinophils, neutrophils and macrophages was observed in PAF-induced animal models.

Conclusion FNF-12 was able to control the inflammatory responses in in vitro and in vivo asthma models, which may be driven by controlling M2-related Th2 cytokines via MAPK and NF- κ B signaling.

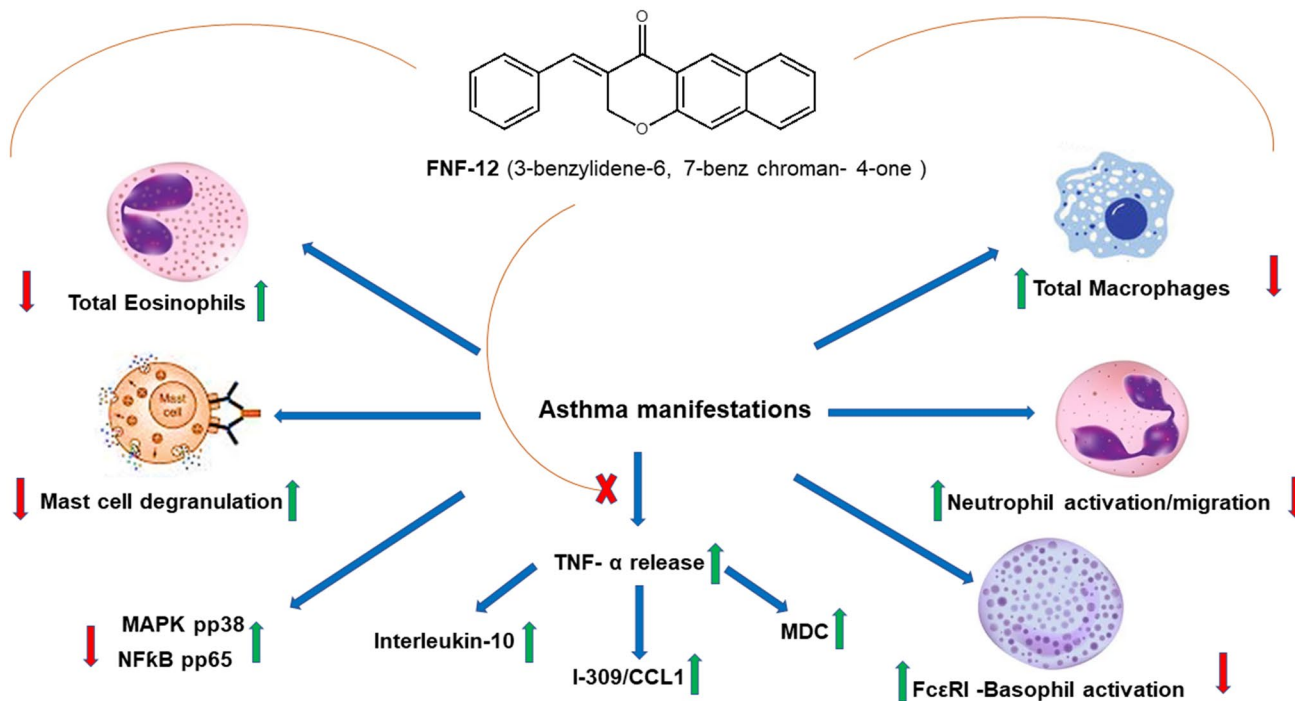
✉ Prasanna Rajagopalan
prachu.rg@gmail.com; rajagopalan@kku.edu.sa

¹ Department of Clinical Laboratory Sciences, College of Applied Medical Sciences, King Khalid University, Abha, Saudi Arabia

² Central Research Laboratory, Department of Clinical Laboratory Sciences, College of Applied Medical Sciences, King Khalid University, Abha, Saudi Arabia

³ Post Graduate and Research Department of Chemistry, Presidency College, Chennai, Tamil Nadu, India

Graphic abstract



Keywords Asthma · Benzylidene-chromanone · MAPK-NF- κ B · Platelet activation factor · Th2 cytokines

Abbreviations

ACD solution	Citrate–dextrose solution
Avidin–HRP	Avidin–horseradish peroxidase
BAL	Bronchoalveolar lavage
DMSO	Dimethylsulphoxide
DNP–BSA	2,4-Dinitrophenol–bovine serum albumin
ELISA	Enzyme-linked immunosorbent assay
EMEM	Eagle's minimum essential medium
fMLP	<i>N</i> -Formyl-methionyl-leucyl-phenylalanine
HBSS	Hank's balanced salt solution
HWB	Human whole blood
IgE	Immunoglobulin E
LPS	Lipopolysaccharide
MAPK	Mitogen-activated protein kinase
MPO	Myeloperoxidase
MTT	3-(4,5-Dimethylthiazol-2-yl)-2,5-diphenyl-2H-tetrazolium bromide
NF- κ B	Nuclear factor kappa B
NMR	Nuclear mass resonance
PAF	Platelet activation factor
PBS	Phosphate-buffered saline
PE	Phycocerythrin
PIPES	Ethanesulphonic acid
RBL-2H3	Rat basophilic leukemia

THP-1	Acute monocytic leukaemia
TNF- α	Tumor necrosis factor- α

Introduction

Asthma is a chronic inflammatory disorder of the airways employing an array of cells and elements [1]. Early onset of the disease affects 20% of the world population with an increasing trend in developed countries [2]. Allergen exposures may worsen the asthmatic symptoms through synergistic cascade mediated by pollution and respiratory infections [3]. Asthma is also reported to be accommodated with airway inflammatory conditions that include, but not limited to, wheezing, breath problems and cough that are generally reversed upon treatment [4].

At bronchial level, asthma is characterized by chronic airway inflammation where cytokines play an active role involving the TH2 cells [5], thereby attracting T cells as a successful target in asthma treatment. On the other hand, the nasal responses of allergy involves immunoglobulin E (IgE) proteins which are predominately found on the surfaces of basophils and mast cells [6]. Activation of the ubiquitous nuclear factor (NF)-kappa B (NF- κ B) transcription factor through phosphorylation is an important event in the inflammatory process

[7]. A study by Zhu et al. in 2019 showed the involvement of NF- κ B-p65 activation in asthma [8]. Similarly, eosinophils and neutrophils are responsible for the production of eotaxins and myeloperoxidase (MPO), respectively, which have been shown to be elevated in allergic conditions [8]. These data support the idea that neutrophilic and eosinophilic infiltrations are the major pathogenic processes in asthmatic progression. Furthermore, involvement of NF- κ B is also connected with neutrophilic and eosinophilic infiltrations of asthmatic reactions [9, 10]. The mitogen-activated protein kinase (MAPK) and NF- κ B pathways are shown to regulate inflammatory immune responses in asthma [11] via Th2 responses [12]. Recently, Fengjuan et al. showed that NF- κ B-p65 translocation and the p38 phosphorylation of MAPK as a hallmark control of the IgE signalling in inflammatory mediators of asthma [13]. When the IgE receptors are cross-linked, the allergic phase of the mast cells is initiated via proinflammatory cells such as eosinophils, neutrophils, lymphocytes, and epithelial cells [6]. Taking into account all the aforesaid manifestations of asthmatic reactions, in this study, we mimicked IgE-mediated mast cell degranulation in RBL-2H3 cells, along with the human blood cell-derived neutrophils/basophils for screening and evaluation of novel compound against asthmatic manifestations linking the MAPK- and NF- κ B signalling.

The major drawback with current treatments for asthma is the resumption of symptoms when the treatment is withdrawn. While glucocorticoids may be beneficial, resistance to these drugs stands as a major pitfall in asthma treatments. On this context, the search of novel agents in asthma management proves beneficial. The 3-benzylidene chroman-4-one moiety occupies a special place in the field of oxygen heterocycles, as this structural feature forms an integral part of many natural products and biologically active molecules [14]. There is a close resemblance of chromanones to naturally occurring compounds such as flavanones, flavones, chromones and coumarins. The biological activity of these naturally occurring compounds with a chroman ring system [15] suggested the synthesis of 4-chromanones [16]. The common occurrence of basic side chains in therapeutically active compounds is deemed worthwhile to incorporate basic group into chromanones to evaluate biological activities. Therefore, we evaluated 3-benzylidene-6,7-benz-chroman-4-one (FNF-12), a novel benzylidene-chromanone moiety, for its efficacy in *in vitro* and *in vivo* models of asthma.

Materials and methods

Materials

4-Methylumbelliferyl-beta-D-glucuronide, anti-2,4-dinitrophenol-bovine serum albumin (DNP-BSA), PAF, anti-DPN IgE antibody and other chemicals were procured from

Sigma-Aldrich [St. Louis, USA]. RBL-2H3 cell line from ATCC [American Type Culture Collection, Rockville, MD, USA]. p-p38 MAPK (Thr180, Tyr182)-PE, p-NF κ B p65 (S529) PE and ELISA kits were purchased from e-Bioscience/Thermo Fisher [San Diego, USA]. The Flow CAST[®] kit was purchased from Buhlmann Diagnostics Corp [Amherst, NH, USA]. Migration inserts, 96-wells plates were obtained from Nunc corp. [NY, USA]. Twenty ml of heparinized human whole blood (HWB) was collected from the blood bank [College of Applied Medical Sciences, King Khalid University, KSA] from eight different donors and used for whole blood analysis and neutrophil isolations. FLUOstar Omega Microplate Reader from BMG LABTECH [Ortenberg, Germany] was used to read absorbance. Guava easy-Cyte[™] flow cytometer [Millipore Corp, USA] with an built-InCyte software was used for flow cytometry analysis.

Methods

FNF-12 chemistry

¹H NMR spectra were recorded in CDCl₃ on a JEOL spectrometer (500 MHz) using SiMe₄ as internal reference and mass spectra were recorded in JEOL.DX-303 spectrometer. ¹³C NMR spectra were recorded using a 100 MHz NMR instrument. For ¹H NMR, 10 mg of compound was dissolved in between 0.6 and 1 mL of solvent in CDCl₃ so that the sample depth was at least 4.5 cm in the tube. For ¹³C NMR, 10–50 mg of sample was used. Infrared (IR) spectra were recorded by the KBr pellet method in a Thermo Mattson Satellite model FTIR spectrophotometer. The EI mass spectra were recorded using a JEOL DX-303 spectrometer.

Ethical clearance

Use of human blood and animal experiments were approved in accordance by the Research Ethics Committee, King Khalid University (HAPO-06-B-001), Abha, Saudi Arabia (Reference No. ECM#2020-3219), dated 12-10-2020 and were conducted according to their guidelines.

Cell culture

Eagle's minimum essential medium (EMEM) was used for the growth of RBL-2H3. RPMI 1640 medium was used to grow human monocytic cell line THP-1. Cells were grown as per standard protocols in growth media supplemented with 10% FBS, 100 U/mL of penicillin, and 100 U/mL streptomycin.

Cell viability assay

Prior to assessing the influence of FNF-12 on RBL-2H3 cells, the cytotoxicity of the compound in these cells were analysed by 3-(4,5-dimethylthiazol-2-yl)-2,5-diphenyl-2H-tetrazolium bromide (MTT) assay as described elsewhere [17]. Briefly, 5000 cells/well, RBL-2H3 cells were grown in regular 96-well cell culture plates with 100 μ L of regular growth media. After overnight incubation, 10–3000 nM of FNF-12 was added to the cells and further incubated for 24 h at 37 °C. Dimethylsulphoxide (DMSO) was used as blank control. To check out the viability of cells in the presence of DNP-BSA, another set of RBL-2H3 cells were pre-incubated for 1 h with 10–3000 nM FNF-12, with suitable blank and activated for 4 h with DNP-BSA. After these incubation periods, both plates were treated similarly for MTT assay. Briefly, after removing the medium, 100 μ L of MTT [1 mg/mL] was added to the wells and incubated for 4.5 h. Formazan products were dissolved in 200 μ L of DMSO, and the absorbance was measured at 560 nm. Percent cell viability was calculated using GraphPad Prism (6.0) software.

IgE-stimulated degranulation and TNF- α estimation in RBL-2H3 cells

IgE-degranulation in RBL-2H3 cells was analysed by following the protocol as described previously by Naal et al. [18]. RBL-2H3 cells sensitized with 1 μ g/mL IgE were seeded at a concentration of 2×10^5 cells/mL in 24-well plates and incubated overnight at 37 °C. The medium was replaced with piperazine-N,N'-bis(2-ethanesulphonic acid (PIPES) buffer (containing NaCl 1.64 g, KCl 74.55 gm, glucose 198.00 mg, MgCl₂ 24.4 mg, CaCl₂ 22.2 mg, PIPES 0.64 gm, BSA 200.00 mg dissolved in 200 mL MilliQ water, with pH adjusted to 7.4) and the cells were further incubated at 37 °C for 15 min. Respective concentrations (0.1–3000 nM) of FNF-12 were added, and cells were incubated at 37 °C for 1 h. DMSO was used as a blank. Then, 0.025 μ g of anti-DNP-BSA was added and incubated for 4 h in a CO₂ incubator. After a brief centrifugation at 448 RCF for 5 min, 50 μ L of supernatant from each well was incubated with 200 μ L of fluorescence substrate (3.79 mg, 4-methylumbelliferyl-beta-D-glucuronide prepared in 10 mL of citrate buffer) at 37 °C for 1 h. Fluorescence intensity was read at 450 nm (emission) and 360 nm (excitation). Supernatants were used for tumor necrosis factor α (TNF- α) estimation by enzyme-linked immunosorbent assay (ELISA) as per the manufacturer's instructions.

Isolation of neutrophils from human whole blood

Neutrophil isolation from human whole blood was performed by dextran sedimentation-based density gradient

centrifugation using citrate–dextrose solution (ACD solution) with some modifications [19]. Human whole blood, ACD solution, and 6% dextran sulphate were incubated at RT for 60 min at 4 °C to separate the yellowish supernatant. The supernatant was centrifuged at 148 RCF for 12 min. 0.6 M KCl was added to the pellet and centrifuged at 189 RCF. HiSep density gradient was used to separate the cells, which were collected in ice cooled Hank's balanced salt solution (HBSS) buffer containing 0.0003 M Na₂HPO₄·2H₂O, 0.0004 M, KH₂PO₄, 0.006 M D-glucose (dextrose) and 0.004 M NaHCO₃ (pH 7.4). Density was adjusted to 2×10^5 cells /mL for further neutrophil-based assays.

Neutrophil elastase assay

This assay was performed in accordance with the protocol established by Ioana et al. with some modifications [20] as follows. Neutrophils (49 μ L) were added to 96-wellsplate and treated with 10, 25, 50 and 100 nM of FNF-12 or DMSO. Master mix containing 10 μ M N-formyl-methionyl-leucyl-phenylalanine (fMLP), 200 μ g/mL cytochalasin-B, 1 mM sodium azide, and 1 mg/mL L-methionine was used to induce the neutrophils, which was further incubated for 1.5 h. at 37 °C. Plates were centrifuged at 448 RCF for 5 min at room temperature (RT). In a fresh plate, 90 μ L of supernatant was transferred to each well and added with 10 μ L of 10 mM elastase substrate, followed by an incubation period for 1 h at 37 °C. The color developed was read spectrophotometrically at 410 nm.

Neutrophil migration inhibition assay

Neutrophil migration was assessed by a protocol as described previously [21]. To a 24-well plate, 249 μ L of HBSS buffer was added, followed by 1 μ L of 10 nM of fMLP. The neutrophil cell suspension was added to inserts and placed on these wells. 249 μ L of 1 μ L of DMSO or 10, 25, 50 and 100 nM of FNF-12 was applied and the neutrophils were allowed to migrate for 1.5 h at 37 °C in a CO₂ incubator. Inserts were stained with crystal violet solution, eluted, and absorption was quantified spectrophotometrically at 410 nm.

IgE-Fc ϵ RI–basophil activation test [BAT assay] in human whole blood

Basophil activation was assessed using Flow CAST[®] assay kit (Buhlmann Diagnostics Corp, USA) as per the manufacturer's instructions. 50 μ L of whole blood in the centrifuge tube was incubated with 1–1000 nM FNF-12 for 20 min at RT. 5 μ L of anti-IgE-Fc ϵ RI was added to the tubes. A mixture of 100 μ L and 20 μ L of stimulation buffer and staining reagent was added, respectively. Post-incubation in the dark

for 15 min, cells were centrifuged at 1792 RCF for 10 min, the supernatant was removed and the remainder suspended with 1 mL PBS. Cell counts were acquired using Guava easyCyte flow cytometer. Percentage CD63-positive cells were determined using InCyte software and IC₅₀ value was presented.

THP-1 cells differentiation and cytokine assays

THP-1 cells were centrifuged at 252 RCF for 5 min. After resuspension in fresh media, 5×10^5 /mL cells were seeded in 24-well plates for 24 h before use for experiments. THP-1 cells were cultured with 20 ng/mL PMA (phorbol 12-myristate 13-acetate) and 20 ng/mL IL-4 for 3 days for M2 macrophage polarization [22]. THP-1-derived M2 macrophages were pretreated with 10, 50, 100 or 150 nM of FNF-12 2 h prior to 0.25 µg/mL LPS induction. After 48 h, the plates were centrifuged at 1792 RCF for 10 min, and the supernatant was kept at -80 °C. ELISA was performed per manufacturer's instructions. Briefly, 100 µL capture antibody was pre-coated to the ELISA plates, washed and incubated overnight at 4 °C. After addition of samples to the wells, the plates were incubated at 4 °C overnight. The contents were discarded and the wells were washed with 200 µL of wash buffer, for five times, 15 s each. 100 µL of detection antibody was added to wells and incubated at room temperature for 1 h. Then, the wells were washed as before and added with 100 µL of avidin-horseradish peroxidase (avidin-HRP) and incubated at room temperature for 30 min. Post five washes, 100 µL of TMB solution was added and the plates were incubated at RT for 15 min. The colour formation was terminated with 50 µL of stop solution, absorbance read at A450 nm and A570 nm, and IC₅₀ was calculated using Graphpad Prism software (6.0).

Flow cytometry for signalling proteins

Key cellular proteins were detected by flow cytometry in THP-1-derived M2 macrophages treated with 10, 50, 100 or 150 nM of FNF-12 for 2 h. Then, cells were induced with 0.25 µg/mL LPS for 30 min. Cells were harvested, washed twice with sterile PBS and incubated with 0.25 µg/mL of NFκB-phycoerythrin (NFκB-PE) or 0.10 µg p-p38 MAPK (Thr180, Tyr182) PE-tagged antibody for 15 min. After washing the cells two times with phosphate-buffered saline (PBS), the cells were re-suspended in HBSS buffer. Ten thousand events were acquired on a Guava easyCyte™ flow cytometer. Data were analysed using In Cyte software (Millipore) to determine the percentage of positive cells.

Animal studies

Animals Thirty Male guinea pigs (Dunken Hartley-strain), age of 10–12 weeks, weighing 325–375 g were used in the study. Guinea pigs were maintained under controlled conditions (18–22 °C, 55 ± 10 humidity, 12 h day/night cycle) and fed a standard diet and water.

Test compound 1 mg of FNF-12 was weighed and transferred to a mortar. 125 µL of Polysorbate 80 (Merck, Gibbstown, NJ) was added to the mortar and triturated to get a smooth paste. 50 mL of 0.5% w/v methyl cellulose (Merck, Gibbstown, NJ) was added in gravimetric dilution fashion and triturated to get a fine suspension.

Grouping and dosing A total number of 30 guinea pigs were randomized and divided into five groups ($n = 6$). The grouping and dosing of animals are briefly indicated by figure number 8. Ear pinnae were marked with an indelible marking pen for identification. Ct were induction control animals. Sh were untreated sham. Group 3–5 were FNF-12-treated animals. On day 0, weights were recorded and fasted animals were treated with test compounds orally. G1 received 0.25 mg/kg FNF-12. G2 animals received 0.5 mg/kg FNF-12, while G3 animals were administered with 1 mg/kg FNF-12. Ct animals were treated with 0.5% w/v methylcellulose (0.5 g methylcellulose was dissolved in 100 mL milliQ H₂O) which served as the vehicle. Sh animals were left untreated. 1 h after compound administration, Ct, G1, G2 and G3 animals were nebulized with platelet activation factor PAF (Sigma, St. Louis, MO) for 10 min using ultrasonic nebulizer with flow rate of 0.25 mL per min (100 µg PAF/animal).

Sample collection and analysis 24 h after treatments, bronchoalveolar lavage (BAL) fluid samples were collected and analysed for total and differential leukocyte count. Samples were centrifuged (1200×g for 10 min) and the resulting cell pellet was resuspended in 0.2 mL of PBS. The total number of white blood cells was determined in (BAL fluid using a haemocytometer. Total cell count was presented as 10⁶ cells. Differential cell count was calculated manually. One hundred microliters of the cell suspension was centrifuged using cytospin chamber to prepare a cell smear. The cell smear was stained with a Giemsa staining solution (0.5%) for differentiation and microscopically observed to identify cells according to their morphological characteristics. The number of each cell types and control-normalized percentage inhibition of the cells in different groups were presented.

Statistical analysis

The experiments were performed in triplicate and all data were represented the mean \pm SD. Graphpad Prism (6.0) [La Jolla, USA] was used for statistical examinations. Results were expressed as the mean \pm SD. GI₅₀/IC₅₀ values were calculated using a non-linear regression fit model with variable slope and plotted accordingly. One-way analysis of variance (one-way ANOVA) was used to check any significant differences in the results of experimental trial, followed by Tukey's post hoc test for multiple comparisons. Significance level 0.05 or 95% confidence interval was used. *p* values of * \leq 0.05; ** \leq 0.01 and *** \leq 0.001 were considered significant.

Results

FNF-12 chemistry

Proton NMR (¹H NMR) and carbon nuclear magnetic resonance spectroscopy (¹³C NMR) from Fig. 1a and b show sharp IR absorption at 1665, 1596 cm⁻¹ and the disappearance of broad band around 3430 cm⁻¹, indicating an aromatic unsaturated ketone. Spectrum doublet in the PMR at 9.45 δ for a single proton indicates the lone vinylic proton. A doublet at 7.95 δ for two protons, a doublet at 7.77 δ for one proton, a doublet of a triplet at 7.68 δ for one proton, and another doublet of triplet at 7.45 δ for one proton, a

quartet at 7.28 δ for four protons, a doublet at 7.09 δ for one proton indicate ten aromatic protons. A doublet at 5.4 δ for two protons indicates the naphthoxy-methylene protons. From the mass spectroscopy (Fig. 1c) inference, the *m/e* value of the compound corresponds to the molecular weight of 286.32. Elemental analysis agree with the molecular formula of compound with Calcd: C, 83.98%; H, 4.93%; found: C, 83.99%; H, 4.94%. From these data, the compound was identified to be 3-benzylidene-6,7-benz-chroman-4-one (Fig. 1b) and internal reference for the compound was given as FNF-12.

Toxicity effects of FNF-12 on normal and stimulated RBL-2H3 cells

The viability of RBL-2H3 cells was unaltered up to 500 nM of FNF-12 treatment (Fig. 2a) at 24 h, while 1000 nM and 3000 nM showed reduction in cell viability when compared to untreated control, [one-way ANOVA, $F(6, 21) = 28.28$, $r^2 = 0.88$, $df = 6$, $p < 0.0001$]. To check out the cytotoxic effect of FNF-12 on IgE stimulation, different doses of FNF-12 were assessed on 1 μ g/mL anti-DNP IgE antibody pre-sensitized RBL-2H3 cells, in the presence of 0.025 μ g/mL DNP-BSA for 4 h. No toxic effects were observed up to 500 nM of FNF-12 concentration [one-way ANOVA, $F(7, 40) = 32.40$, $r^2 = 0.85$, $df = 7$, $p < 0.0001$] (Fig. 2b). Therefore, concentrations less than 500 nM of FNF-12 were decided to be tested for activity in the presence or absence of IgE-DNP-BSA.

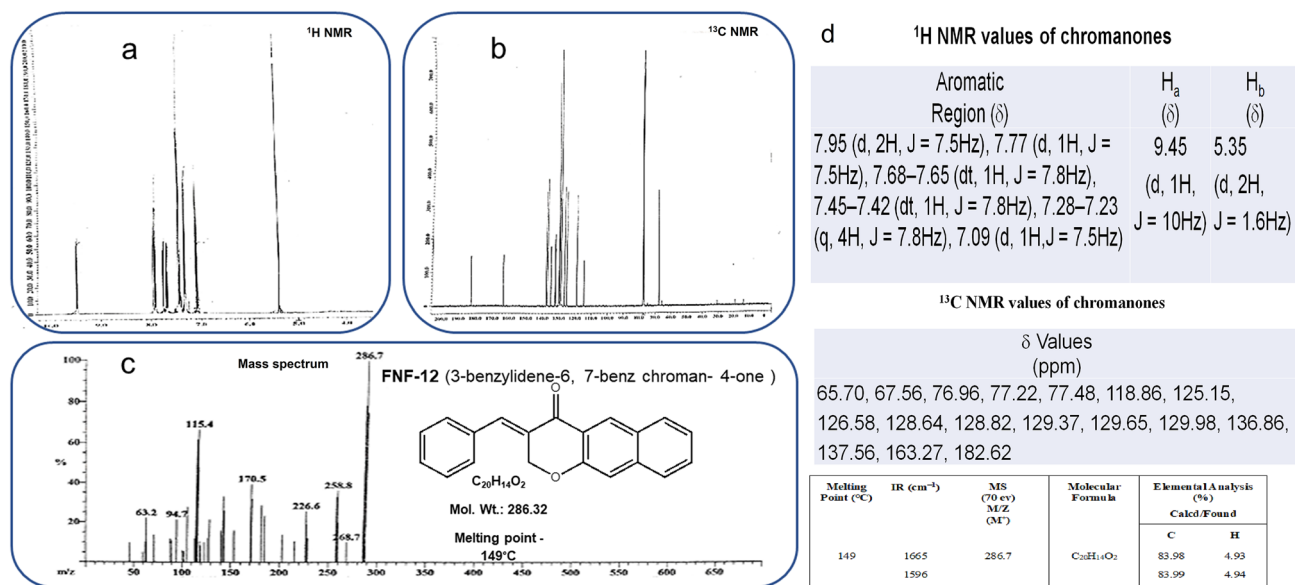


Fig. 1 Chemistry profiling of FNF-12. **a** Proton NMR of the synthesized compound. **b** Carbon nuclear magnetic resonance spectroscopy of FNF-12. **c** Mass spectrum confirming the structure, molecular

weight and IUPAC name of the synthesized compound FNF-12. **d** δ values based on NMR results and elemental analysis depicting physical and chemical properties of the compound

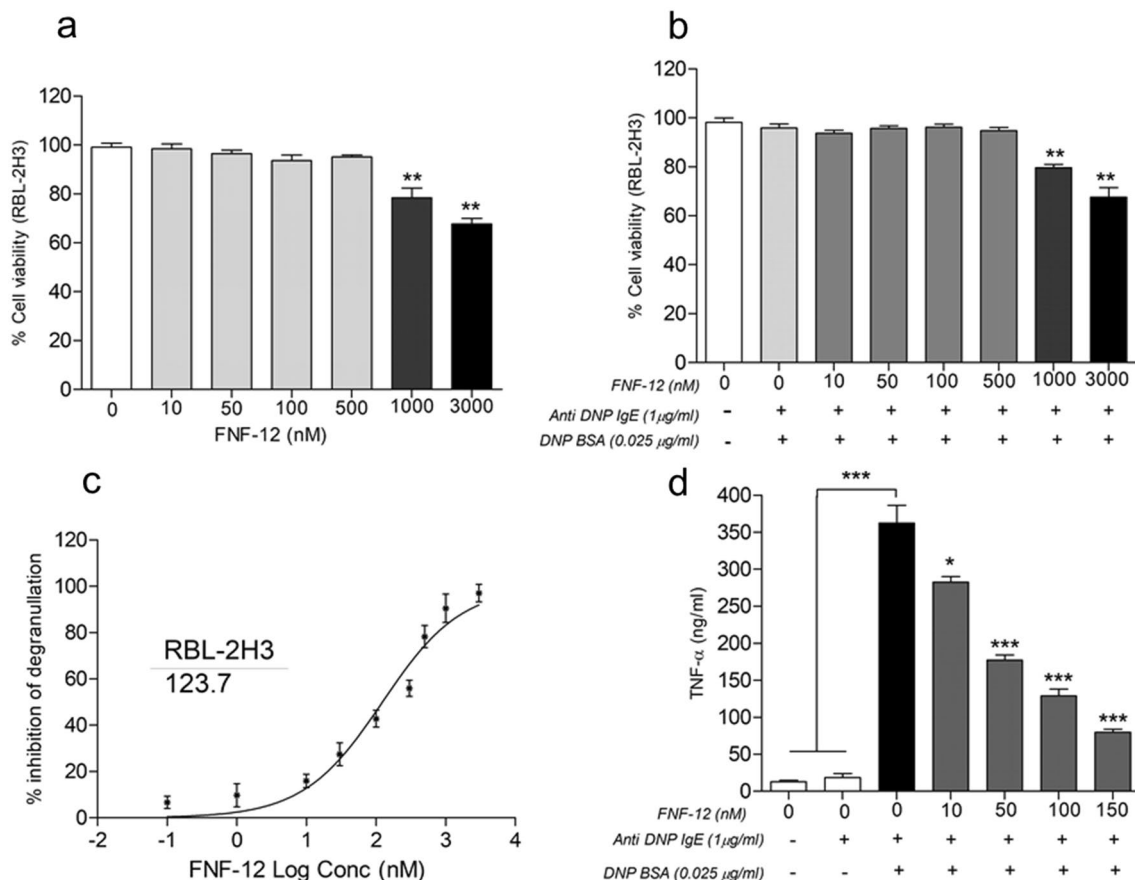


Fig. 2 Cytotoxicity indices for FNF-12 at different concentrations in **a** normal RBL-2H3 cells and **b** anti-DNP IgE-sensitized RBL-2H3 cells with DNP-BSA induction. Cell viability was measured by MTT assay. Dose-dependent cytokine/degranulation inhibitory profile of FNF-12 in anti-DNP IgE-sensitized RBL-2H3, stimulated by DNP BSA. RBL-2H3 cells were sensitized overnight and pre-incubated with different concentrations of FNF-12 for 1 h and stimulated with DNP-BSA for 4 h. The results were expressed as mean \pm SD, analysed by one-way ANOVA followed by Tukey's multiple com-

parison test. $** \leq 0.01$. **c** RBL-2H3 cell degranulation in supernatant was assessed fluorimetrically as a measure of β -glucuronidase release using 4-methylumbelliferyl-beta-D-glucuronide substrate. Results are expressed as the mean \pm SD and IC_{50} values were determined by GraphPad prism (6.0) software. **d** TNF- α was measured in the supernatants of RBL-2H3 cells in the presence or absence of FNF-12. Results expressed as mean \pm SD, analysed by one-way ANOVA, followed by Tukey's multiple comparison test. $* \leq 0.05$ and $*** \leq 0.001$

FNF-12 repressed degranulation and TNF- α release in sensitized RBL-2H3 cells

RBL-2H3 cells were pre-sensitized to anti-DNP IgE and then stimulated with DNP-BSA for degranulation. We assessed the release of β -glucuronidase, using a fluorescent substrate to assess the effect of FNF-12 on degranulation inhibition. FNF-12 dose-dependently controlled RBL-2H3 degranulation with an IC_{50} value of 123.7 nM (Fig. 2c). ELISA was used to measure TNF- α release inhibition in RBL-2H3 cells. A dose-dependent reduction in TNF- α release (Fig. 2d) [one-way ANOVA, $F(6, 21) = 150.1$, $r^2 = 0.97$, $df = 6$, $p < 0.0001$] in cell supernatant was evident with FNF-12 treatment.

FNF-12 effectively reduced neutrophil activity

FNF-12 inhibited the elastase exocytosis of activated neutrophils in a dose-dependent manner [one-way ANOVA, $F(4, 25) = 258.2$, $r^2 = 0.97$, $df = 4$, $p < 0.0001$] (Fig. 3a). Likewise, the compound dose-dependently inhibited neutrophil migration under the influence of the chemoattractant [one-way ANOVA, $F(4, 25) = 199.0$, $r^2 = 0.96$, $df = 6$, $p < 0.0001$] (Fig. 3b).

Effect of FNF-12 on activated basophils

Human whole blood basophils were activated by cross-linking the IgE-Fc ϵ RI receptors and further stimulating them

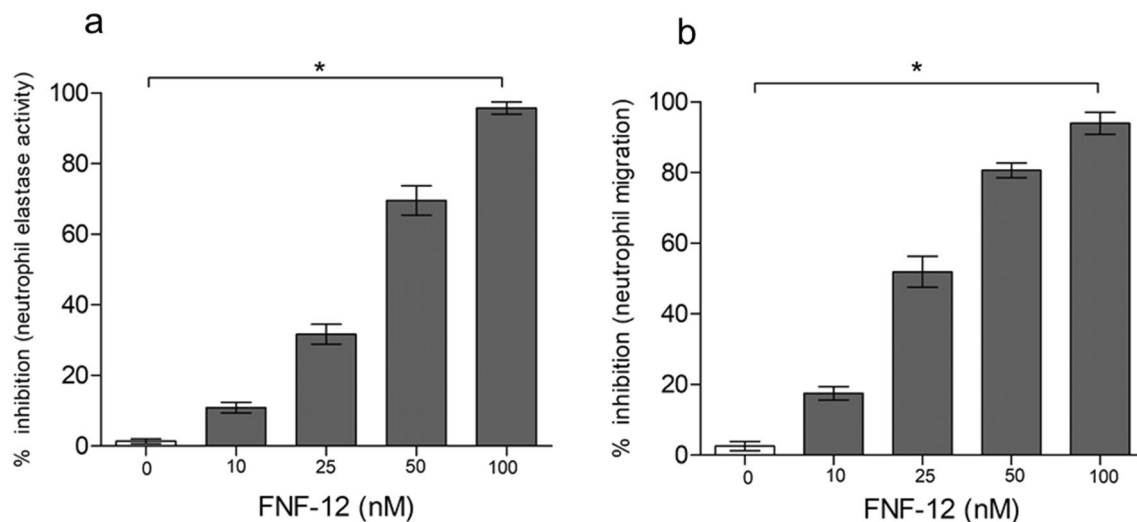


Fig. 3 Inhibitory profile of FNF-12 on neutrophil action. FNF-12 dose-dependently inhibited **a** neutrophil elastase and **b** migration exocytosis. Results are expressed as mean \pm SD, analysed by one-way

ANOVA, followed by post hoc comparisons using the Tukey HSD multiple comparison test. * \leq 0.05

with anti-IgE monoclonal antibodies. Once stimulated, these cells expressed CD63 surface receptors, which were then measured by flow cytometry. CCR3 positivity was used for gating the CD63-positive populations. The results demonstrated a suppression of basophil activation as evidenced by decrease in the CD63 cell population when compared to the untreated control. The IC_{50} value was found to be 205 nM (Fig. 4).

FNF-12 reduced cytokine/chemokine expressions, THP-1 derived M2 macrophages

To determine the effect of FNF-12 on cytokine/chemokine expressions, THP-1-derived M2 macrophages were pre-treated with 50 nM, 100 nM and 150 nM FNF-12 treatments of FNF-12 for 2 h prior to 0.25 μ g/mL LPS induction. Inference from our results indicated dose-dependent suppression of IL-10 [one-way ANOVA, $F(5, 18) = 82.62$, $r^2 = 0.95$, $df = 5$, $p < 0.0001$] (Fig. 5a), I-309/CCL1 [one-way ANOVA, $F(5, 18) = 39.61$, $r^2 = 0.91$, $df = 5$, $p < 0.0001$] (Fig. 5b) and MDC/CCL22 expressions [one-way ANOVA, $F(5, 18) = 31.26$, $r^2 = 0.89$, $df = 5$, $p < 0.0001$] (Fig. 5c). However, no significant effect in suppression of the tested protein levels was evident at 10 nM treatment to the THP-1-derived M2 macrophages (Fig. 5a–c).

FNF-12 suppressed MAPK and NF κ B signals in LPS-induced M2 macrophages

To analyse the involvement of key signalling proteins involved in LPS-induced IL-10, I-309/CCL1, and MDC/

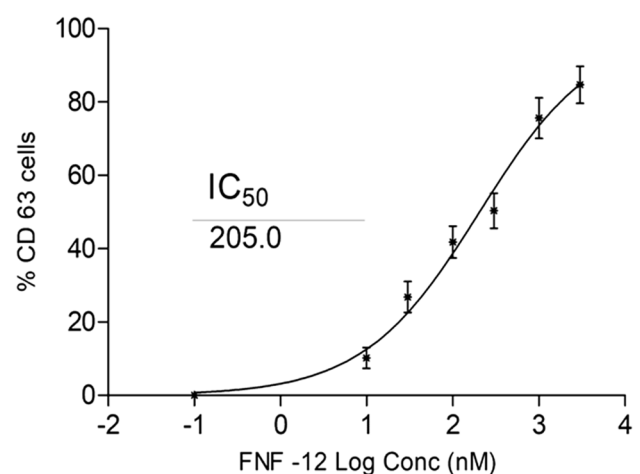


Fig. 4 Inhibitory effects of different concentrations of FNF-12 on activated basophils stimulated by anti-Fc ϵ RI monoclonal antibody. Basophil activation was evaluated from CD63-expressed positive cells gated from CCR 3-positive population. IC_{50} of FNF-12 was analysed for CD 63-positive cells by GraphPad Prism (6.0) software

CCL22 production in THP-1-derived M2 macrophages, we investigated the effects of FNF-12 on the pp-38 expression of the MAPK and pp-65 expression of NF κ B by flow cytometry. Our results demonstrated a dose-dependent reduction in expression of pp-38 MAPK protein upon LPS induction with FNF-12 treatments (Fig. 6). Similarly, a dose-dependent decrease in pp-65 NF κ B expression was observed in these cells from 10 to 150 nM FNF-12 treatments (Figs. 7, 8).

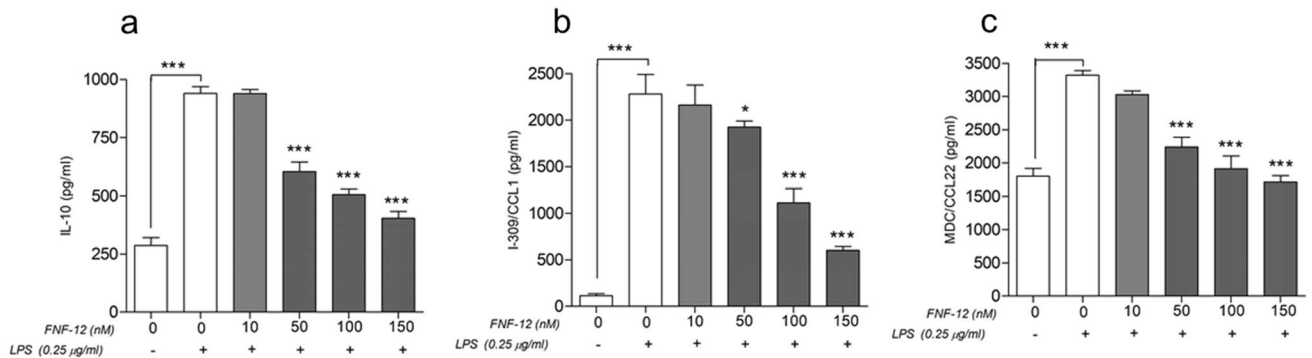


Fig. 5 Effects of FNF-12 on expression levels of **a** IL-10, **b** I-309/CCL1, and **c** MDC/CCL22 in THP-1-derived M2 macrophages. Different concentrations of FNF-12 were pretreated for 2 h to the THP-1-M2 macrophages and further induced with 0.25 mg/mL LPS for 48 h. FNF-12 dose-dependently suppressed IL-10, I-309/CCL1,

and MDC/CCL22 expressions from 50 nM dose. Data represent the mean \pm SD, analysed by one-way ANOVA followed by post hoc comparisons using the Tukey HSD multiple comparison test. * ≤ 0.05 and *** ≤ 0.001

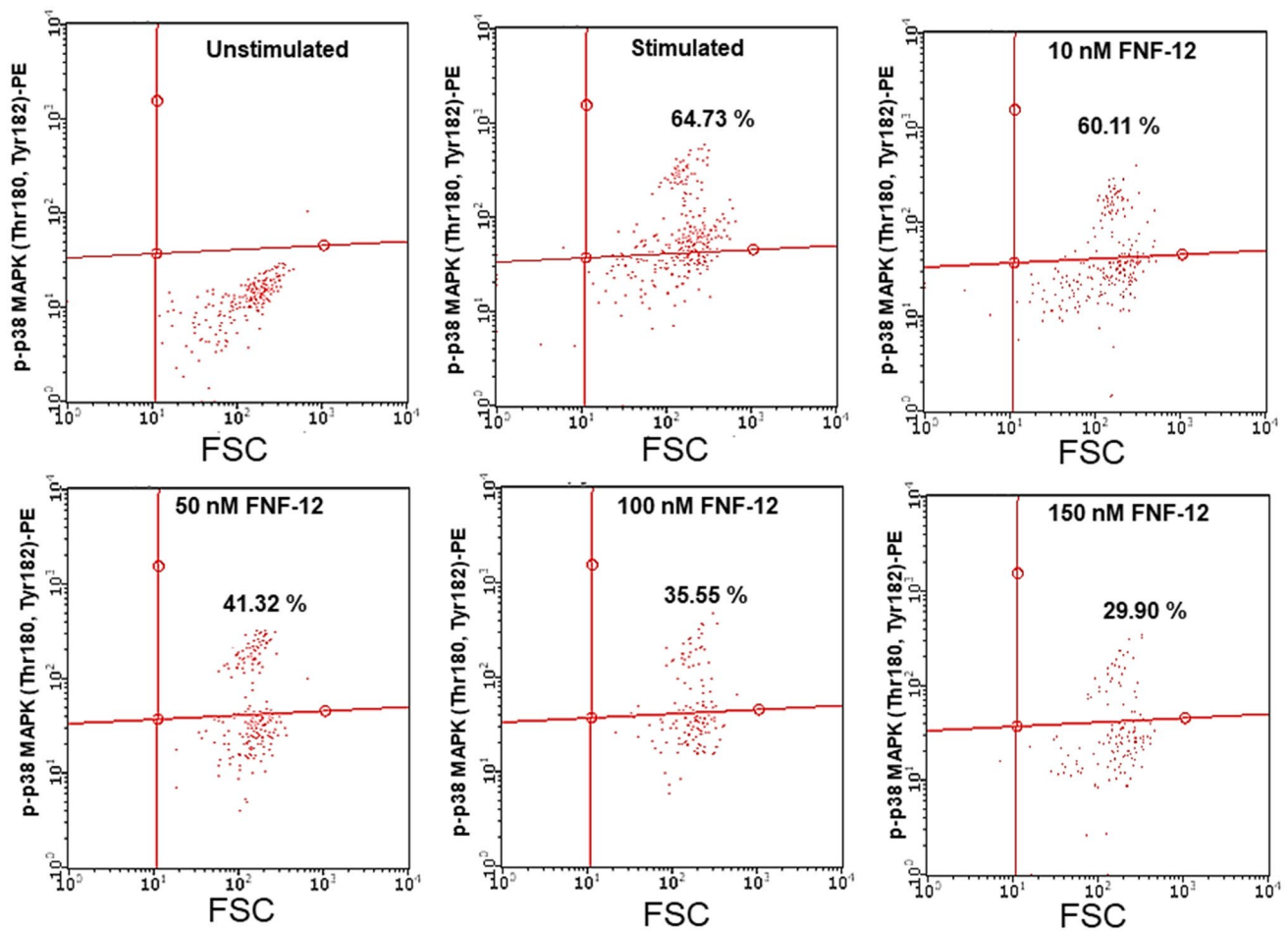


Fig. 6 Flow cytometry evaluations of MAPK signalling with FNF-12 treatment and LPS induction. FNF-12 downregulated LPS-induced MAPK p-p38 in a dose-responsive way

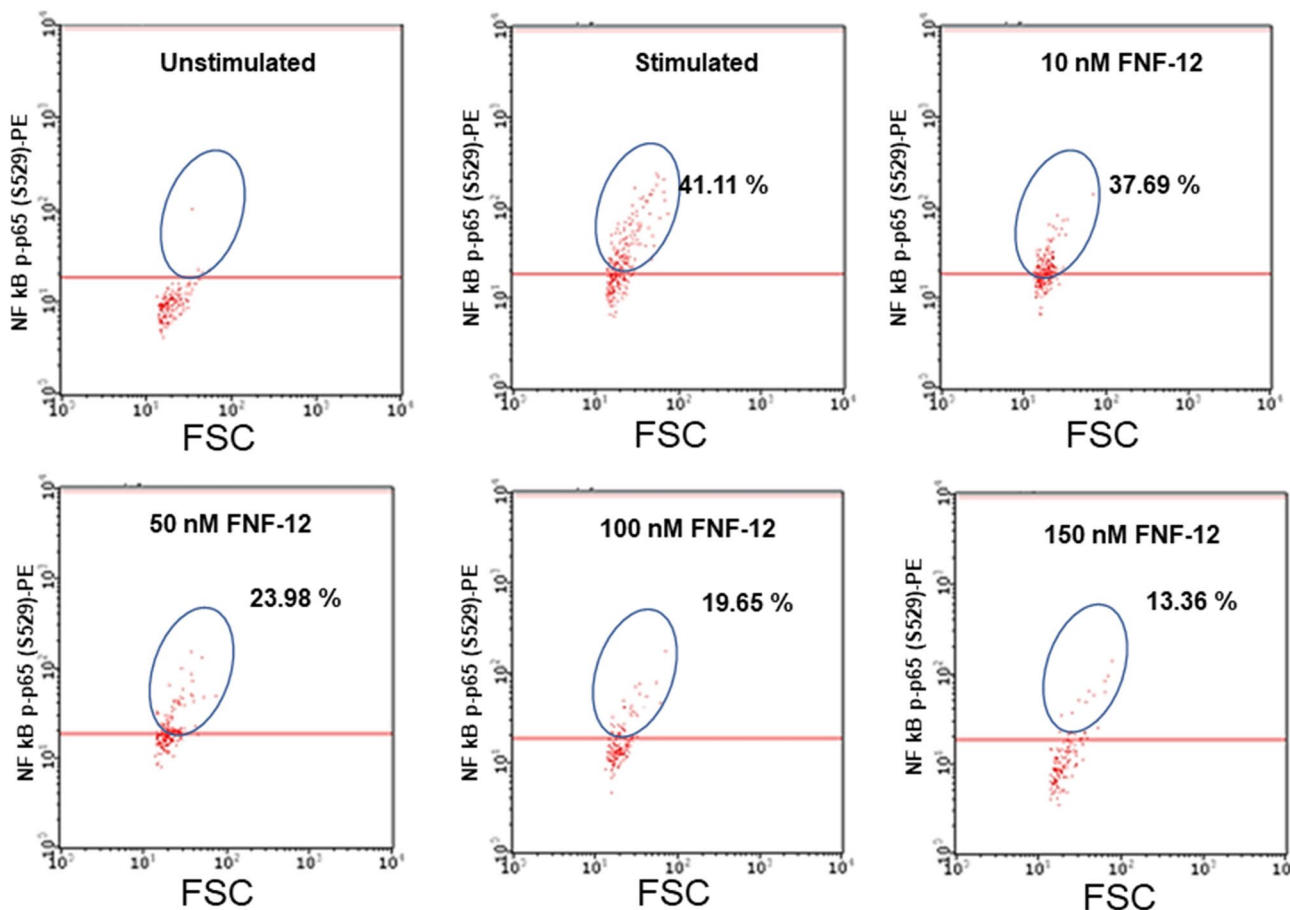
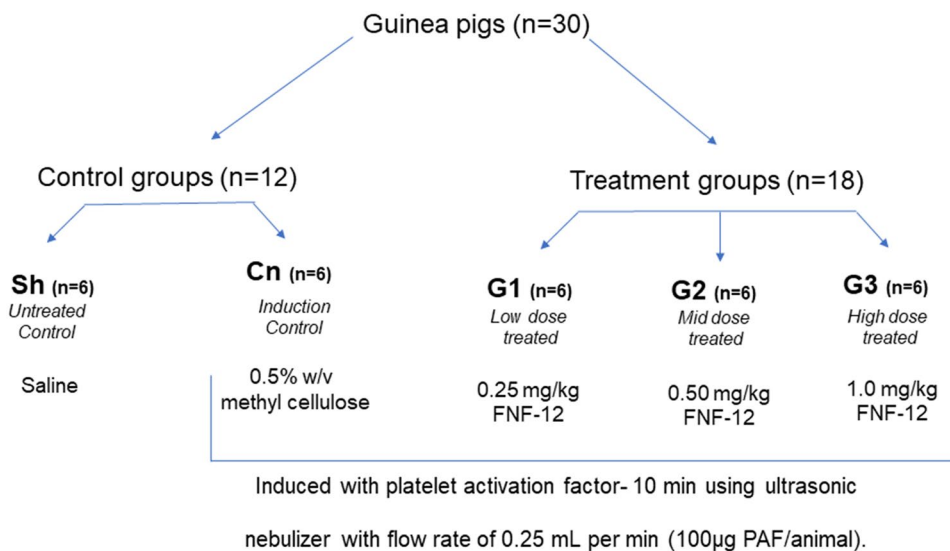


Fig. 7 Evaluations of NFκB signalling with FNF-12 treatment under influence of LPS induction. FNF-12 reduced the NFκB p-p65 expressions from 10 to 150 nM concentrations

Fig. 8 Schematic representation of experimental design, grouping and drug treatment schedule



Effects of FNF-12 on platelet activation factor-induced guinea pig asthma model

Next, to assess the transformation of the observed in vitro activity of FNF-12 in the in vivo asthma model, we used PAF to induce asthmatic response with respect to leucocytes, eosinophils, neutrophils and macrophages in guinea pigs. In Cn animals, the accumulation or infiltration of leucocytes was observed to be 6.17 ± 1.06 , when compared to 0.61 ± 0.05 Sh animals (Fig. 9a). In the treated group, G1 and G2 animals showed leucocyte counts of 5.19 ± 0.50 ; 4.42 ± 0.78 , respectively (Fig. 9a). With 1 mg/kg FNF-12 treatment for the G3 group, the leucocyte counts further significantly reduced to 1.25 ± 0.48 [one-way ANOVA, $F(4, 24) = 14.08$, $r^2 = 0.70$, $df = 4$, $p < 0.0001$] (Fig. 9a). In Cn animals, the infiltration of eosinophils was observed as 1.21 ± 0.24 , when compared to Sh which had 0.02 ± 0.002 (Fig. 9b). G1, G2 and G3 animals depicted a significant dose-dependent reduction in eosinophil accumulation with values of 0.94 ± 0.12 ; 0.47 ± 0.18 and 0.39 ± 0.3 , respectively [one-way ANOVA, $F(4, 24) = 19.18$, $r^2 = 0.76$, $df = 4$, $p < 0.0001$] (Fig. 9b). A similar significant reduction in the

neutrophil [one-way ANOVA, $F(4, 24) = 13.96$, $r^2 = 0.69$, $df = 4$, $p < 0.0001$] (Fig. 9c) and macrophage counts [one-way ANOVA, $F(4, 24) = 18.24$, $r^2 = 0.76$, $df = 4$, $p < 0.0001$] (Fig. 9d) was observed with increasing FNF-12 doses (G1–G3) when compared with Cn animals.

Discussion

3-Benzylidene-chromanones are an important class of small molecules that resemble natural active compounds like flavanones and polyphenols with potent biological activities [23]. 3-Benzylidene-4-chromanones have proven antimicrobial activities [24]. The same class of compounds exhibited excellent antioxidant activity by inhibiting α -glucosidase enzymes [25]. 3-Benzylidene-7-methoxy-chroman-4-one derivatives have been proven for their anticancer efficacies against human breast and neuroblastoma cancer cells [26]. With such promising background of this class of compound, the current study focused on evaluating novel 3-benzylidene-chroman-4-one derivatives for their activities for immunomodulatory effects in in vitro and in vivo asthma models.

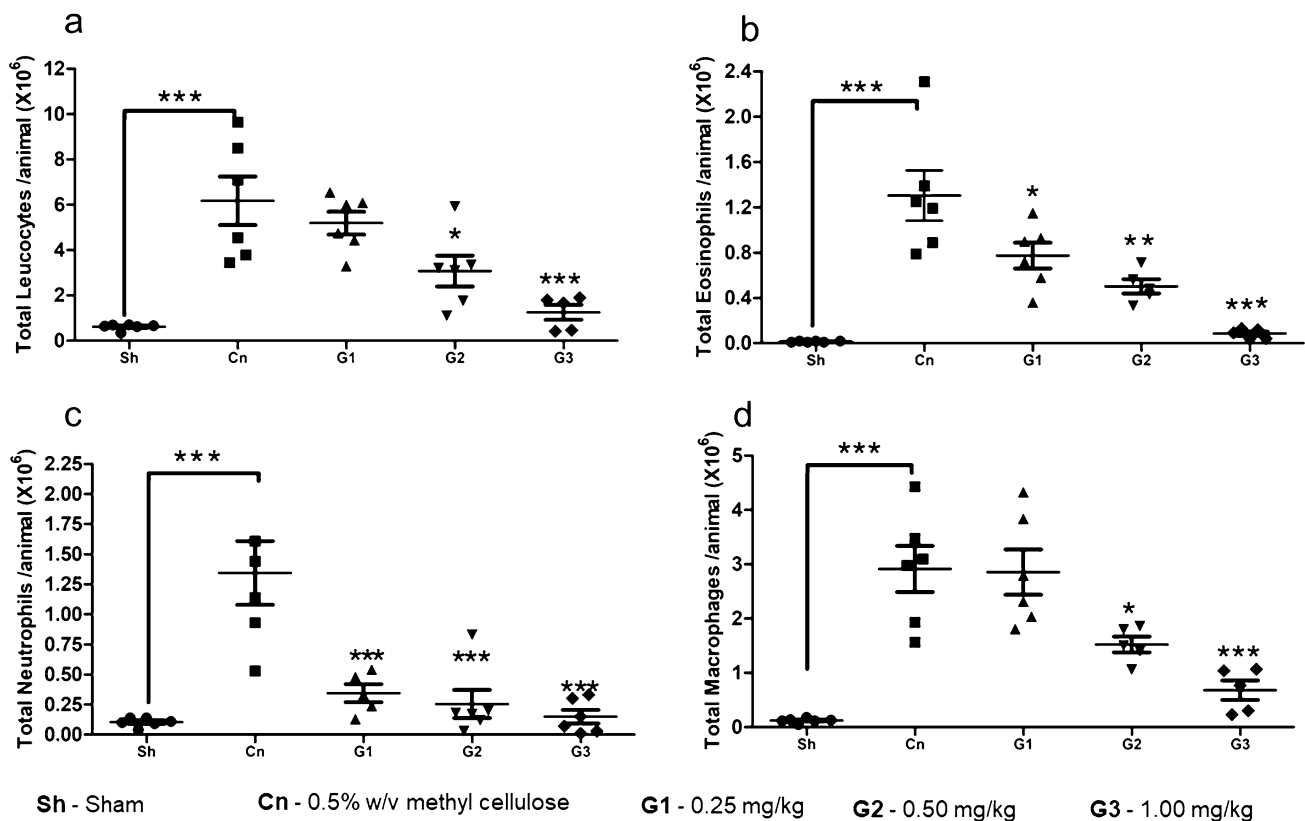


Fig. 9 Immunology profiling of FNF-12-treated platelet-activating factor-induced guinea pig asthma model. FNF-12 dose-dependently suppressed **a** total leucocytes, **b** eosinophils, **c** neutrophils and **d** macrophages when compared with nontreated control group. The

results were analysed by one-way ANOVA followed by post hoc comparisons using the Tukey HSD multiple comparison test to compare Cn with Sn and treated groups (G1–G3). * ≤ 0.05 ; ** ≤ 0.01 and *** ≤ 0.001

Based on the preliminary *in vitro* screening, FNF-12 was identified as a lead molecule, which was further evaluated for activity against asthmatic manifestation models in this study.

Products of mast cells is shown to centrally mediate the airway components. During the asthmatic process, the mast cells are recruited by air way-smooth muscles which in turn contribute to the responsiveness via secondary mediators like cytokines and histamine [27]. Further to the hyperresponsiveness, the activated mast cells also has a control on the proliferation and remodelling of airway epithelial cells [28]. The cytokines derived from the activated mast cells aids in the differentiation of the TH2 cells which in turn initiates the allergen-specific IgE cascade which are mediated by the B cells [29]. Followingly, activation of basophils, mast cells, and downstream stimulation of neutrophils are all commonly driven by IgE mediated mechanisms. Therefore, we evaluated the effect of FNF-12 on these effector cells. Our results demonstrated a dose dependent activity of FNF-12 in controlling IgE mediated mast cell degranulation, thereby indicating the efficacy of the molecule in controlling the asthmatic effector reactions. Prior to evaluate the biological efficacy of FNF-12, we checked for the cytotoxicity of the compound in mast cells with both sensitized and un sensitized cells. The observed non-toxicity of FNF-12 at biologically active concentrations complemented to the tretaputic safety of the molecule.

Neutrophils are the primary effector cells in inflammatory reactions. Involvement of neutrophils in type 2 allergic asthma is well documented [30], where neutrophil elastase (NE) contribute to the manifestations of asthmatic exacerbations [31]. On the other hand, studies show TNF- α as the prime proinflammatory cytokine, which aid in rolling and adhesion of neutrophils for recruitment at the inflammation site [32]. The current study demonstrated a dose dependent inhibition in elastase and migration activities of neutrophils by FNF-12, which was in par with the aforesaid literature. Further, efficacy of FNF-12 in controlling TNF- α release in activated mast cells suggested the involvement of this cytokine in controlling mast cell and neutrophil activities. Expression of CCR3 + CD63 positive population is regarded as a direct measure for basophil activation expressing IgE-Fc ϵ RI receptors. Our observations indicated FNF-12 to dose dependently suppress the activation of basophils. As it is documented that mast cell-derived mediators produced by Fc ϵ R1 cross-linking with allergen can lead to recruitment, adhesion and activation of leucocytes [28], the observed activity of FNF-12 in suppressing the neutrophil and basophil activation can be linked to IgE-Fc ϵ RI mediated process.

The role of macrophages in chronic diseases like asthma cannot be sidelined. Asthmatic inflammation is characterized by the enrolment of Th2 lymphocytes, which in turn drive

many cytokines to influence airway macrophages toward alternative (M2) polarization [33]. Melgert et al. showed M2 macrophages to be elevated in both bronchoalveolar lavage fluid and airway tissue of asthmatic patients which could aggravate inflammation [34]. We therefore evaluated the effects of FNF-12 in Th2 cytokines with human monocytic THP-1 derived M2 macrophages. Our observations showed that FNF-12 was capable of suppressing IL-10, I-309/CCL1 and MDS expressions in these cells when stimulated with LPS. These observations were in agreement to other studies which shows anti-inflammatory effects in asthmatic models via suppression of Th2 cytokines [35, 36].

NF- κ B, is a well-known redox-sensitive transcription factor that constitutes an important role in the broad spectrum of inflammatory networks via regulation of cytokine activity in airway pathology [37]. NF- κ B, is also considered an ideal proinflammatory marker [38]. As far as asthma is concerned, hyper activation of NF- κ B was reported in the bronchial biopsies and inflammatory cells of COPD individuals [38]. TNF α -stimulated cytokine release from PBMCs of COPD was shown in asthmatic patients [39]. Further, the neutrophils in the sputum of COPD-asthmatic patients showed increased NF- κ B signalling [40]. Previous studies indicate the involvement of NF- κ B in monocytes/macrophages, by generating of proinflammatory cytokines [41]. *In vivo*, genetic targeting of NF- κ B intermediates has been reported to attenuate airway inflammation in response to lipopolysaccharide (LPS) [42, 43]. The observed decrease in expression of M2-related IL-10, I-309 /CCL1 and MDS and alteration of the neutrohil action in this study can therefore be linked with the interference of NF- κ B signalling. On the other hand, MAPK signalling pathway constitute a central driving processes in many immune responses [44]. Analysis indicated a dose responsive reduction of MAPK p-p38 under influence of LPS-stimulation. A tight correlation between MAPK and NF- κ B pathway has been reported for chemokine release in bronchial inflammation [45]. Phosphorylated MAPK (MAPK-P38) targets a number of kinases, transcription factors and cytoskeletal proteins to infer inflammatory effects [46]. p38 MAPK activation increases inflammation by stabilizing mRNA transcripts of some cytokines, such as TNF α [46]. MAPK activation at p38 is shown to potentiate the proinflammatory effects of NF- κ B by phosphorylation [47]. Overall, these evidences are in support to our observation of FNF-12 acting via MAPK-p38-NF- κ B signalling mediated by M2-related Th2 cytokines.

To infer if our *in vitro* results are translated *in vivo*, we used PAF-asthma model to evaluate FNF-12 efficacy. PAF is a naturally occurring phospholipid mediator produced by a variety of inflammatory cells including neutrophils, alveolar macrophages, mast cells, eosinophils, and others [48]. PAF originates from cleavage of membrane phospholipids

by phospholipase A2 yielding lyso-PAF, which is further acetylated to form biologically active PAF [49]. Besides broncho-constriction, activation of eosinophils and airway hyperresponsiveness, PAF is also actively involved in mucus hyper-secretion which is a critical feature during asthma [50]. PAF has been shown to serve as a powerful mucus secretagogue in the airways of animals and humans [50]. The mechanism of PAF induced airway hypersecretion has been extensively studied during the last years and accumulating evidence supports the notion that the pulmonary effects of PAF could be mediated by the secondary release of leukotrienes [51]. It has also been established that inhalation or intratracheal instillation of PAF can induce a selective accumulation of effector cells like eosinophils [52]. These observations raise the possibility that inhibition of eosinophil accumulation may be a property common to anti-asthma drugs. Many different molecules activate eosinophils to release various chemokine and cytokine mediators including Th2 [53]. A study showed that lung eosinophil apoptosis was significantly delayed in asthmatic patients mediated via NF- κ B activation [54]. Studies show that mice with deficient NF- κ B could not mount eosinophilic airway inflammatory responses and also had a decreased Th2 production when compared to wild-type mice. Taken together, these observations the hypothesis that NF- κ B is a central inflammatory factor that drives severe eosinophilic asthma, which could be a potential therapeutic target to prevent eosinophilia [55, 56]. Our results also demonstrate the eosinophil accumulation in BALF within 24 h inhalation of 100 μ g/animal PAF. There was an increase in the percentage of eosinophils 24 h after inhalation of PAF compared to BSA-saline challenged Sh group, while FNF-12 treatments controlled eosinophil accumulation in a dose-responsive way. In accordance with the in vitro observations, FNF-12 also controlled the accumulation of other effector cells like neutrophils and macrophages, which exhibited the efficacy of this candidate in controlling PAF-induced asthmatic manifestations. While our preliminary observations support the efficacy of FNF-12, a detailed mechanistic investigation with more parameters of airway inflammation is a limitation, which is recommended as future directions for this study.

Conclusion

In summary, FNF-12 demonstrated efficacy in controlling the inflammatory responses in in vitro and in vivo asthma models which may be driven by controlling M2-related Th2 cytokines via MAPK and NF- κ B signaling. Further research is recommended to develop this novel compound against asthmatic manifestations.

Acknowledgements The authors express their gratitude to SMART-BIO LABS, Chennai, Tamil Nadu, India, for the help rendered in this study.

Author contributions MA—funding, experimental, data curing. MAS—data analysis, statistical analysis, experimental. MYA—experimental, manuscript preparation. NB—data analysis, revision of manuscript. SR—experimental, data analysis, reference management. PR—conceptual design, data analysis, manuscript finalization, supervision.

Funding The authors extend their thanks to the Deanship of Scientific Research at King Khalid University, Abha, Saudi Arabia, for funding this work through Grant number RGP. 1/265/42.

Declarations

Conflict of interest The authors declare that there is no conflict of interest related to this study.

References

- Mizgerd JP. Lung infection—a public health priority. *PLoS Med.* 2006;3:e76.
- Asher MI, Montefort S, Björkstén B, Lai CK, Strachan DP, Weiland SK, et al. Worldwide time trends in the prevalence of symptoms of asthma, allergic rhinoconjunctivitis, and eczema in childhood: ISAAC phases one and three repeat multicountry cross-sectional surveys. *Lancet.* 2006;368:733–43.
- Spannhake EW, Reddy SP, Jacoby DB, Yu XY, Saatian B, Tian J. Synergism between rhinovirus infection and oxidant pollutant exposure enhances airway epithelial cell cytokine production. *Environ Health Perspect.* 2002;110:665–70.
- Edwards MR, Bartlett NW, Clarke D, Birrell M, Belvisi M, Johnston SL. Targeting the NF-kappaB pathway in asthma and chronic obstructive pulmonary disease. *Pharmacol Ther.* 2009;121:1–13.
- Wenzel SE. Asthma: defining of the persistent adult phenotypes. *Lancet.* 2006;368:804–13.
- Green RM, Custovic A, Sanderson G, Hunter J, Johnston SL, Woodcock A. Synergism between allergens and viruses and risk of hospital admission with asthma: case-control study. *BMJ.* 2002;324:763.
- Athari SS. Targeting cell signaling in allergic asthma. *Signal Transduct Target Ther.* 2019;4:45.
- Zhu L, Chen X, Chong L, Kong L, Wen S, Zhang H, et al. Adiponectin alleviates exacerbation of airway inflammation and oxidative stress in obesity-related asthma mice partly through AMPK signaling pathway. *Int Immunopharmacol.* 2019;67:396–407.
- Catz SD, Johnson JL. Transcriptional regulation of bcl-2 by nuclear factor kappa B and its significance in prostate cancer. *Oncogene.* 2001;20:7342–51.
- Ajuwon KM, Spurlock ME. Adiponectin inhibits LPS-induced NF-kappaB activation and IL-6 production and increases PPAR-gamma2 expression in adipocytes. *Am J Physiol Regul Integr Comp Physiol.* 2005;288:R1220–5.
- Qiu YY, Wu Y, Lin MJ, Bian T, Xiao YL, Qin C. LncRNA-MEG3 functions as a competing endogenous RNA to regulate Treg/Th17 balance in patients with asthma by targeting microRNA-17/ROR γ t. *Biomedicine & pharmacotherapy (Biomedicine & pharmacotherapie).* 2019;111:386–94.

12. Shieh YH, Huang HM, Ching-Chiung W, Lee CC, Fan CK, Lee YL. Corrigendum to "Zerumbone enhances the Th1 response and ameliorates ovalbumin-induced Th2 responses and airway inflammation in mice" [Int. Immunopharmacol. 24 (2015) 383-391]. Int Immunopharmacol. 2017;50:371.
13. Yuan F, Liu R, Hu M, Rong X, Bai L, Xu L, et al. JAX2, an ethanol extract of *Hyssopus cuspidatus* Boriss, can prevent bronchial asthma by inhibiting MAPK/NF- κ B inflammatory signaling. Phytomed Int J phytother phytopharmacol. 2019;57:305-14.
14. Takao K, Yamashita M, Yashiro A, Sugita Y. Synthesis and biological evaluation of 3-benzylidene-4-chromanone derivatives as free radical scavengers and α -glucosidase inhibitors. Chem Pharm Bull. 2016;64:1203-7.
15. Livingstone R. Naturally occurring oxygen ring compounds. Nature. 1963;200:509.
16. Kabbe H-J, Widdig A. Synthesis and reactions of 4-chromanones. Angew Chem Int Ed Engl. 1982;21:247-56.
17. Dera A, Rajagopalan P. Thymoquinone attenuates phosphorylation of AKT to inhibit kidney cancer cell proliferation. J Food Biochem. 2019;43:e12793.
18. Naal RM, Tabb J, Holowka D, Baird B. In situ measurement of degranulation as a biosensor based on RBL-2H3 mast cells. Biosens Bioelectron. 2004;20:791-6.
19. Maqbool M, Vidyadaran S, George E, Ramasamy R. Optimisation of laboratory procedures for isolating human peripheral blood derived neutrophils. Med J Malays. 2011;66:296-9.
20. Craciun I, Fenner AM, Kerns RJ. *N*-Arylacetyl *O*-sulfonated aminoglycosides as novel inhibitors of human neutrophil elastase, cathepsin G and proteinase 3. Glycobiology. 2016;26:701-9.
21. Dera A, Rajagopalan P, Ahmed I, Alfihili M, Alsughayyir J, Chandramoorthy HC. Thymoquinone attenuates IgE-mediated allergic response via pi3k-Akt-NF κ B pathway and upregulation of the Nrf2-HO1 axis. J Food Biochem. 2020;44:e13216.
22. Chanput W, Mes JJ, Savelkoul HF, Wichers HJ. Characterization of polarized THP-1 macrophages and polarizing ability of LPS and food compounds. Food Funct. 2013;4:266-76.
23. Raju BC, Tiwari AK, Kumar JA, Ali AZ, Agawane SB, Saidachary G, et al. α -Glucosidase inhibitory antihyperglycemic activity of substituted chromenone derivatives. Bioorg Med Chem. 2010;18:358-65.
24. Das U, Lorand T, Dimmock SG, Perjesi P, Dimmock JR. 3-benzylidene-4-chromanones: a novel cluster of anti-tubercular agents. J Enzyme Inhib Med Chem. 2015;30:259-63.
25. Takao K, Yamashita M, Yashiro A, Sugita Y. Synthesis and biological evaluation of 3-benzylidene-4-chromanone derivatives as free radical scavengers and α -glucosidase inhibitors. Chem Pharm Bull (Tokyo). 2016;64:1203-7.
26. Noushini S, Alipour E, Emami S, Safavi M, Ardestani SK, Gohari AR, et al. Synthesis and cytotoxic properties of novel (E)-3-benzylidene-7-methoxychroman-4-one derivatives. Daru J Fac Pharm Tehran Univ Med Sci. 2013;21:31.
27. Méndez-Enríquez E, Hallgren J. Mast cells and their progenitors in allergic asthma. Front Immunol. 2019;10:821.
28. Cruse G, Bradding P. Mast cells in airway diseases and interstitial lung disease. Eur J Pharmacol. 2016;778:125-38.
29. Zhang H, Wang J, Wang L, Zhan M, Li S, Fang Z, et al. Induction of mast cell accumulation by chymase via an enzymatic activity- and intercellular adhesion molecule-1-dependent mechanism. Br J Pharmacol. 2018;175:678-92.
30. Radermecker C, Louis R, Bureau F, Marichal T. Role of neutrophils in allergic asthma. Curr Opin Immunol. 2018;54:28-34.
31. Radermecker C, Sabatel C, Vanwinge C, Ruscitti C, Maréchal P, Perin F, et al. Locally instructed CXCR4(hi) neutrophils trigger environment-driven allergic asthma through the release of neutrophil extracellular traps. Nat Immunol. 2019;20:1444-55.
32. Oliveira SH, Canetti C, Ribeiro RA, Cunha FQ. Neutrophil migration induced by IL-1 β depends upon LTB4 released by macrophages and upon TNF- α and IL-1 β released by mast cells. Inflammation. 2008;31:36-46.
33. Gordon S. Alternative activation of macrophages. Nat Rev Immunol. 2003;3:23-35.
34. Melgert BN, ten Hacken NH, Rutgers B, Timens W, Postma DS, Hylkema MN. More alternative activation of macrophages in lungs of asthmatic patients. J Allergy Clin Immunol. 2011;127:831-3.
35. Lin YC, Huang MY, Lee MS, Hsieh CC, Kuo HF, Kuo CH, et al. Effects of montelukast on M2-related cytokine and chemokine in M2 macrophages. J Microbiol Immunol Infect. 2018;51:18-26.
36. Wu AY, Chik SC, Chan AW, Li Z, Tsang KW, Li W. Anti-inflammatory effects of high-dose montelukast in an animal model of acute asthma. Clin Exp Allergy. 2003;33:359-66.
37. Schuliga M. NF- κ B signaling in chronic inflammatory airway disease. Biomolecules. 2015;5:1266-83.
38. Park EK, Jung HS, Yang HI, Yoo MC, Kim C, Kim KS. Optimized THP-1 differentiation is required for the detection of responses to weak stimuli. Inflamm Res. 2007;56:45-50.
39. Gagliardo R, Chanez P, Profita M, Bonanno A, Albano GD, Montalbano AM, et al. I κ B kinase-driven nuclear factor- κ B activation in patients with asthma and chronic obstructive pulmonary disease. J Allergy Clin Immunol. 2011;128(635-45):e1-2.
40. Brown V, Elborn JS, Bradley J, Ennis M. Dysregulated apoptosis and NF κ B expression in COPD subjects. Respir Res. 2009;10:24.
41. Tahan F, Jazrawi E, Moodley T, Rovati GE, Adcock IM. Montelukast inhibits tumour necrosis factor- α -mediated interleukin-8 expression through inhibition of nuclear factor- κ B p65-associated histone acetyltransferase activity. Clin Exp Allergy. 2008;38:805-11.
42. Li YT, He B, Wang YZ, Wang J. Effects of intratracheal administration of nuclear factor- κ B decoy oligodeoxynucleotides on long-term cigarette smoke-induced lung inflammation and pathology in mice. Respir Res. 2009;10:79.
43. Rajendrasozhan S, Hwang JW, Yao H, Kishore N, Rahman I. Anti-inflammatory effect of a selective I κ B kinase- β inhibitor in rat lung in response to LPS and cigarette smoke. Pulm Pharmacol Ther. 2010;23:172-81.
44. Dong C, Davis RJ, Flavell RA. MAP kinases in the immune response. Annu Rev Immunol. 2002;20:55-72.
45. Wong CK, Wang CB, Ip WK, Tian YP, Lam CW. Role of p38 MAPK and NF- κ B for chemokine release in coculture of human eosinophils and bronchial epithelial cells. Clin Exp Immunol. 2005;139:90-100.
46. Barnes PJ. Kinases as novel therapeutic targets in asthma and chronic obstructive pulmonary disease. Pharmacol Rev. 2016;68:788-815.
47. Saccani S, Pantano S, Natoli G. p38-Dependent marking of inflammatory genes for increased NF- κ B recruitment. Nat Immunol. 2002;3:69-75.
48. Kasperska-Zajac A, Brzoza Z, Rogala B. Platelet-activating factor (PAF): a review of its role in asthma and clinical efficacy of PAF antagonists in the disease therapy. Recent Pat Inflamm Allergy Drug Discov. 2008;2:72-6.
49. Tsukioka K, Matsuzaki M, Nakamata M, Kayahara H, Nakagawa T. Increased plasma level of platelet-activating factor (PAF) and decreased serum PAF acetylhydrolase (PAFAH) activity in adults with bronchial asthma. J Investig Allergol Clin Immunol. 1996;6:22-9.
50. Kuijpers TW, van den Berg JM, Tool AT, Roos D. The impact of platelet-activating factor (PAF)-like mediators on the functional activity of neutrophils: anti-inflammatory effects of human PAF-acetylhydrolase. Clin Exp Immunol. 2001;123:412-20.

51. Stafforini DM. PAF acetylhydrolase gene polymorphisms and asthma severity. *Pharmacogenomics*. 2001;2:163–75.
52. Sanjar S, Aoki S, Boubekeur K, Burrows L, Colditz I, Chapman I, et al. Inhibition of PAF-induced eosinophil accumulation in pulmonary airways of guinea pigs by anti-asthma drugs. *Jpn J Pharmacol*. 1989;51:167–72.
53. Bruijnzeel PL, Rihs S, Virchow JC Jr, Warringa RA, Moser R, Walker C. Early activation or “priming” of eosinophils in asthma. *Schweizerische medizinische Wochenschrift*. 1992;122:298–301.
54. Ilmarinen P, Kankaanranta H. Eosinophil apoptosis as a therapeutic target in allergic asthma. *Basic Clin Pharmacol Toxicol*. 2014;114:109–17.
55. Yang L, Cohn L, Zhang DH, Homer R, Ray A, Ray P. Essential role of nuclear factor kappaB in the induction of eosinophilia in allergic airway inflammation. *J Exp Med*. 1998;188:1739–50.
56. Donovan CE, Mark DA, He HZ, Liou HC, Kobzik L, Wang Y, et al. NF-kappa B/Rel transcription factors: c-Rel promotes airway hyperresponsiveness and allergic pulmonary inflammation. *J Immunol (Baltimore, Md: 1950)*. 1999;163:6827–33.

Publisher's Note Springer Nature remains neutral with regard to jurisdictional claims in published maps and institutional affiliations.